Diagnostic Imaging in European Eastern Countries: a Russian Experience

18

L.S. Namazova-Baranova, A.A. Baranov, I.E. Smirnov, A.V. Anikin, A.N. Getman, A.K. Gevorkyan, N.L. Komarova, O.V. Kustova, O.V. Komarova, E.V. Komarova, and E.V. Antonova

Contents

18.1 Introduction 349
18.2 Nuclear Medicine (NM) 350
18.3 Nuclear Medicine at the Scientific Center of Children's Health (SCCH) 352
18.4 Functional Radionuclide Kidney Examination 354
18.5 Radionuclide Hepatography 357
18.6 Radionuclide Cardiac Pathology Diagnosis 358
18.7 Radionuclide Pulmonary Pathology Diagnosis 363
18.8 Radionuclide Skeletal System Pathology Diagnosis 366
Conclusion 368
Suggested Reading 370

18.1 Introduction

Radiodiagnosis (diagnostic imaging using radiation sources) is one of the key types of diagnosis in current pediatrics. We may trace the development trajectories of how imaging technologies have changed since Wilhelm Conrad Roentgen discovered X-rays only 120 years ago. One of them has consisted in development of external ionizing radiation imaging methods – from plain radiography to high-resolution computed tomography, the second – in introduction of the methods involving external radiation sources not based on the gamma radiation (ultrasonography, MRI). All pediatricians know that the US is safe, highly available, and diagnostically valuable. Thanks to high natural tissue contrast and absence of radiation exposure, MRI may

L.S. Namazova-Baranova (✉) • A.A. Baranov • I.E. Smirnov • A.V. Anikin
A.N. Getman • A.K. Gevorkyan • N.L. Komarova • O.V. Kustova
O.V. Komarova • E.V. Komarova • E.V. Antonova
Scientific Center of Children's Health, Moscow, Russia
e-mail: namazova@nczd.ru

© Springer International Publishing Switzerland 2016

L. Mansi et al. (eds.), *Clinical Nuclear Medicine in Pediatrics*,
DOI 10.1007/978-3-319-21371-2_18

be successfully used even in the youngest children. Finally, the third trajectory consisted in development of the internal radiation source (radionuclides) methods: from gamma-ray chambers to the state-of-the-art positron emission tomography (PET) methods.

Nowadays, large medical centers are equipped with all the high-technology diagnostic systems – from expert US apparatus to modern CT and MR tomographs, as well as modern gamma-ray systems. The amount of data such equipment is capable of providing is extremely large. However, it is difficult for pediatricians to orient themselves in this data glut. Each method features individual advantages and disadvantages, aims and objectives, spheres of application, and possibilities and constraints. We obtain the maximum amount of diagnostic data only when we are able to use a set of methods including any of the methods and compare results. The economic aspect of the issue ought not to be ignored either, which is why ways of optimizing examinations consisting in cost reduction remain top priority.

Whereas rapid development of imaging technologies in the end of the twentieth century and in the beginning of the twenty-first century resulted in higher demand for radiodiagnostic methods using expert equipment (ultrasound systems, digital radiographic systems, CT and MR tomographs) in clinical pediatrics, examinations using radiopharmaceuticals (RPs) remain less common and widely known. Not only patients, but also physicians mystify them. At the same time, these are unique technologies, which help to directly assess condition of the body on the cellular level. The set of these methods is known as *nuclear medicine and molecular imaging* (real-time imaging of processes on the molecular level).

18.2 Nuclear Medicine (NM)

This term has two definitions – a conventional one and a modern one. According to the initial definition, nuclear medicine is a branch of clinical medicine specializing in the use of radionuclide pharmaceuticals for diagnosis and treatment, i.e., the NM method is based not on the externally induced (as in radiographic methods, such as CT or MRI), but on the body-derived radio emission.

According to a more modern and wider definition, NM is a branch of high-technology medicine using radionuclides and other radiation (both ionizing and non-ionizing) sources to treat and diagnose diseases, such as:

1. Radionuclide and other diagnostic methods, including:
   (a) Single-photon emission computed tomography (SPECT)
   (b) Positron emission tomography (PET)
   (c) Non-radionuclide tomographic methods:
      (i) Computed tomography (CT)
      (ii) Magnetic resonance imaging (MRI)
2. Radionuclide and radiation therapy (RT)
3. Radiopharmaceutical (RP) manufacturing technologies
4. Use of charged particle accelerators for generating isotopes and performing radiation therapy

5. Computer technologies of obtaining and storing tomographic images, as well as of planning radiation therapy and other calculations

It ought to be mentioned that information technologies as a set of methods of obtaining, processing, transforming, transferring, and providing data are ingrained in all spheres of nuclear medicine. In tomography, complex software suites are used to obtain images; they obtain information from the tomograph and recover and transform the image to make it more comprehensible for physicians on the screen (Fig. 18.1).

Nuclear medicine has become ingrained into the arsenal of diagnostic means of modern pediatric establishments. Its distinctive feature is functionality of radionuclide methods. Although gamma-ray images do not feature such a high space resolution as CT or MRI images, they are capable of reflecting pathophysiological and metabolic alterations occurring within the body by means of volume RP distribution in the body, as RPs concentrate in certain organs and form hyperfixation foci.

The number of radionuclide examinations (conventional NM) has been doubling every 3–5 years in the developed countries in the recent years; it is now ca. 10 per 1000 persons. Despite intensive development of other instrumental diagnostic methods, this level has not decreased yet due to the fact that radioisotope diagnosis is primarily a functional and biochemical examination and helps to detect many diseases at such early stages when other methods are insufficiently informative.

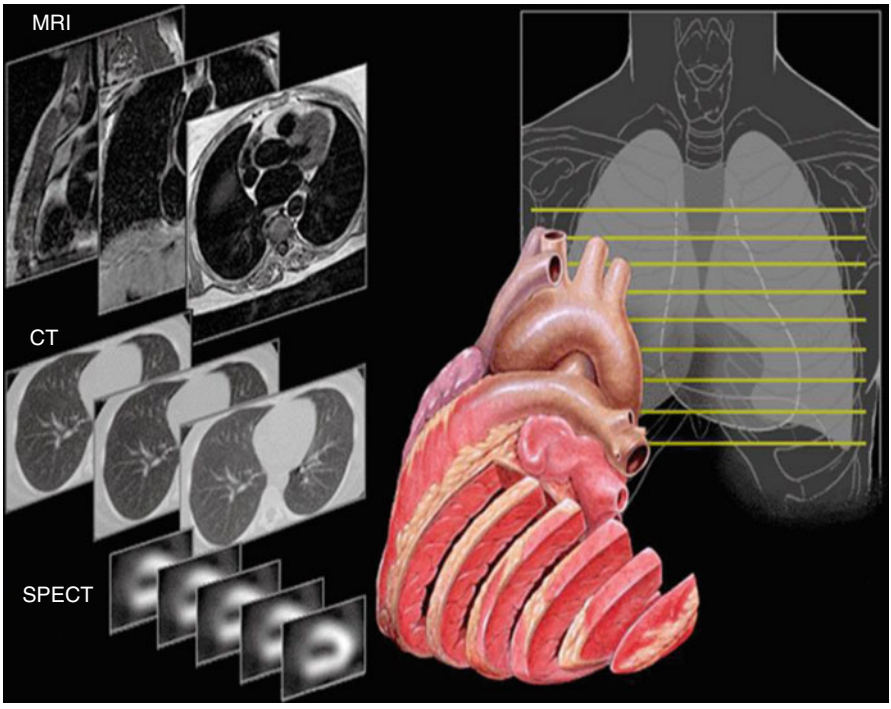

Fig. 18.1 Comparison of magnetic resonance and computed and SPECT tomography images

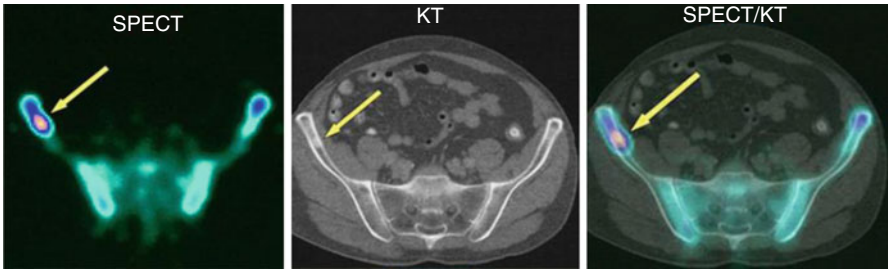

Fig. 18.2 Comparison of SPECT and CT images and a hybrid SPECT/CT image, which helps to determine topography of the pathological focus

Nuclear medicine has been being especially dynamically developed since 1963, when H.O. Anger invented a gamma-ray chamber – a fundamentally new device designed to obtain gamma-ray images, which is based on the use of radionuclide ionizing radiation. The principal design principle of gamma-ray chambers (large flat scintillation crystal with photomultipliers above it) makes the device capable of 3 types of radionuclide examinations: radiometry, radiography, and imaging. Gamma-ray chambers ensure immediate registration of the in vivo administered RP radiation without moving a detector over the patient, high space resolution, and radiation registration rate. Radionuclide imaging (scintigraphy) includes several methods of obtaining images reflecting distribution of labeled compounds within the body. These substances – radiopharmaceuticals (RPs) – are intended to observe and assess visceral physiological functions. According to a range of authors, one of the possibilities of nuclear medicine is creation of body metabolite-based RPs; use of such RPs will provide radionuclide diagnosis with a way to map functional processes and the change rates thereof occurring in a patient's body similar to metabolic pathway maps. In this case RP fixation will demonstrate viability and functional activity of the tissue or organ under analysis.

There are more than 100 radionuclides used to produce RPs for nuclear medicine. However, only technetium-99 m (^{99m}Tc), iodine-123 (^{123}I), as well as thallium (^{201}T1 and ^{199}T1) and gallium (^{67}Ga citrate) nuclides have maintained practical value for radionuclide diagnosis, as their physiochemical and biological properties make them optimal to perform single-photon gamma-ray examinations in children.

Combined SPECT/CT and PET/CT systems have been becoming common in pediatrics in recent years. For example, modern gamma-ray chamber Discovery NM/CT 670 is a combined SPECT/CT system integrated into a single gentry and capable of producing a high-quality combined image of functional and morphological patterns (Fig. 18.2).

18.3 Nuclear Medicine at the Scientific Center of Children's Health (SCCH)

At the moment, the Center has 5 MR tomographs (10.35 T tomograph, 31.5 T tomographs, and 13 T tomograph), 3 multispiral CTs (160–320 slices), more than 20 expert US systems, a digital mammography system (1 MRI of 0.35 T, 3 MRI

- of 1.5 T, 1 MRI - of 3 T), 3 bone densitometers, 5 digital radiodiagnostic systems, and 2 digital angiographs.

The principal technical means of radionuclide diagnosis at the SCCH is expert integrated gamma-ray chamber Millennium MG (USA). In package with a specialized computer system (workstation Xeleris 3) (GE Healthcare, USA), the gamma-ray chamber helps to perform all types of in vivo radionuclide examinations using the standard integrated processes for different data accumulation modes. The examinations performed with such devices are known as single-photon emission computed tomography (SPECT). Whereas X-ray (transmission) tomography is based on obtaining computerized images of body "slices" after processing information on X-ray (external) radiation absorption by tissues, SPECT helps to visualize distribution of the RP administered to the examination subject in the form of two-dimensional planes.

In order to produce RPs we use nuclide generators intended to produce radionuclide pharmaceuticals numerous times directly at the site by means of separating genetically related – parent and daughter – radionuclides. The latter usually has a shorter half-life and is being continuously generated from the parent one. Generators are convenient as the personnel may transport them and subsequently separate the daughter nuclide *ex tempore* directly at a diagnostic laboratory. The most common radionuclide in pediatrics is technetium-99 m (^{99m}Tc) as it has the scintigraphy-perfect monoenergetic gamma radiation spectrum. Use of short-living ^{99m}Tc with half-life of 6 h and soft γ-radiation of 140 keV makes the diagnostic procedure radiologically safe, as it reduces the pediatric patient's radiation exposure tens of times.

We use GT-2 M generators ^{99m}Tc activity of 5.5 GBq on the day of delivery, which ensure generation of an eluate featuring high and stable output of technetium-99 m throughout the lifetime. This nuclide is convenient for clinical use, as it easily forms complexes with the compounds tropic to tissues of various organs. We also use special commercially available vialed lyophilisate sets for clinical practice: technefor (technetium oxabifor), technephyte (technetium phytate), technetril (technetium sestamibi), technemek (technetium succimer), technemag, pentatech (calcium trisodium pentetate), bromezida (mebrofenin) etc. ^{99m}Tc-based RP compounding usually consists in simple concoction of a lyophilisate and the eluate, although specific manipulations may sometimes be required.

The specific apparatus present the obtained data on the dynamics of physiological processes as follows:

- In the quantitative form – number of pulses (scintillations) per image pixel
- In the graphic form – activity/time graphs (radiograms)
- In the form of images (imaging)

According to our data, radionuclide diagnosis is the most informative and cost-effective method of functional examination of various organs with high specificity and sensitivity in pediatrics. Analysis of diagnostic gamma-ray chamber examinations demonstrated that 46 % there of have been scintigraphic examinations of kidneys and urinary organs, 19 % of the liver, 17 % of the heart, 14 % of the lungs, 2.6 % of the skeletal system, and 1.4 % of the thyroid gland and testicles.

18.4 Functional Radionuclide Kidney Examination

Functional radionuclide kidney examination-renograthy which is based on registration of the intravenously administered RP – ^{99m}Tc technemek (DMSA) with activity of 80–600 MBq, which is selectively captured and excreted from kidneys – gamma radiation over kidneys.

Depending on the indication, we take a single image (static mode) or series of consecutive images at different points in time (dynamic mode). Static nephroscintigraphy is used to measure shape, dimensions, and volume of kidneys as well as to determine RP distribution, specific activity, and integral capture index. Dynamic scintigraphy shows activity in the renal microcirculation (perfusion) directly after RP administration, transfer thereof to renal tubules (glomerular filtration) after that, and gradual activity decrease due to urine runoff in the end, which is why it is used to determine the following parameters in children: functional RP distribution ("interest zones"), activity/time curves (renograms), and 2-min capture (indicator of the functioning tissue amount).

Along with that, we have proposed a method of measuring the amount of RP captured by each kidney and both kidneys in tote (RF patent No. 2392968), which helps to rapidly detect the renal functioning tissue amount (FTA) changes in patients with various forms of renal pathologies. This method helps to reduce duration of examination, as the renal FTA measurement requires lower (3.2 times) radiation exposure of the patient and does not require interruption of gamma-ray image recording or radioactive decay correction.

A healthy child's renogram consists of three characteristic segments: segment 1 (vascular), initial steep curve upturn for 40–50 s considered to be a consequence of RP entry into the kidney's vascular system; segment 2 (secretory), subsequent less steep upturn for 3–5 min reflecting RP passage to kidney cavities via tubules; it finishes with the highest curve peak indicating the maximum drug accumulation period (Tmax); after that technemek is gradually excreted to the urinary bladder; hence, segment 3 (excretory) is represented by a steep curve downturn due to RP excretion from the kidney. Excretory segment's duration is calculated on the basis of the drug's half-life – $T_{1/2}$ (normally, up to 12–15 min). The following pathological types of renograms are distinguished depending on the form of renal pathology: obstructive (urinary tract obstruction), parenchymatous (decelerated secretory and excretory renal function in the event of chronic pyelonephritis, hydronephrosis, etc.), isosthenuric (acute secretory and excretory renal malfunction in the event of glomerulonephritis and arteriosclerotic kidney), and afunctional (in the absence of secretory-excretory renal function) (Fig. 18.3).

Examination of children with vesicoureteral reflux (VUR) of different severity detected unilateral and bilateral lesions in 52.6 % and 47.3 % of the cases, respectively. Static nephroscintigraphy helped to detect kidney injuries of different severity in all the examined patients with VUR. A twofold decrease in the affected kidney's functioning parenchyma amount was observed in patients with stage III VUR or worse. The established regularities indicate that the primary factors of the

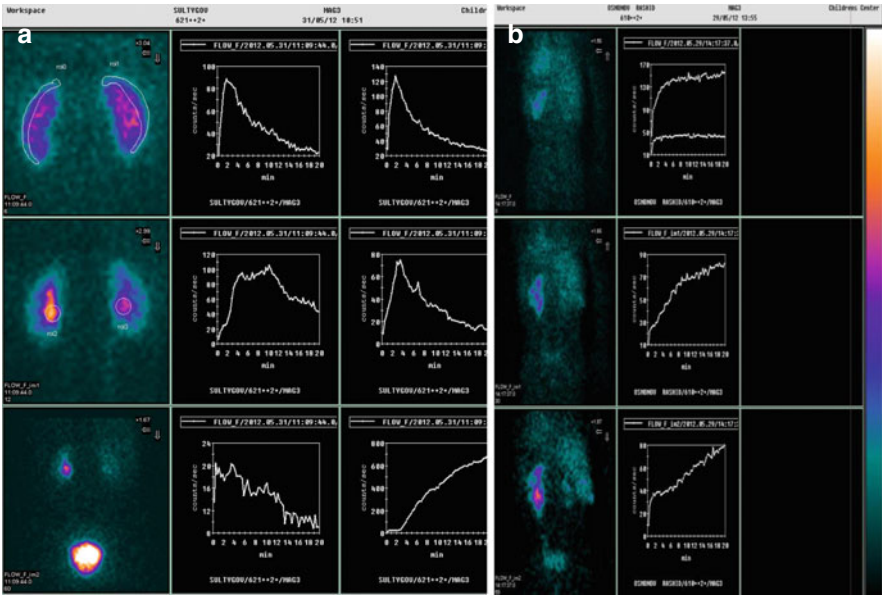

Fig. 18.3 (**a**) Patient S., 14 years of age. Nephroscintigraphy. "Interest zones" in the area of renal parenchyma and pelves, as well as of the urinary bladder. Renogram changes: normal cortical transport, moderately decelerated excretion from the left pelvis, reflux. (**b**) Patient O., 15 years of age. Nephroscintigraphy. Extremely acute depression of the right kidney's function, urodynamic disorders, and CRF

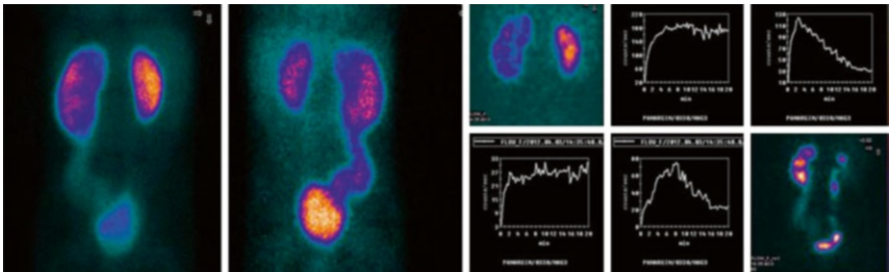

Fig. 18.4 Patient R., 6 years of age. Dynamic nephroscintigraphy 6 months after operative correction of bilateral megaloureter: front view (*left*), back view (*right*). Right kidney's volume (43 cm^3) is lower than normal (75 cm^3). Right kidney's clearance recovery

functional condition of kidneys include not only the reflux grade, but also the nephrosclerosis type or the combination thereof, especially in the event of bilateral VUR in children characterized by significant impairment of the structural-functional condition of kidneys. Nephroscintigraphy also helps to adequately assess reserves of the functionally active renal parenchyma in children with VUR (Fig. 18.4).

Radionuclide examinations of 2–16-year-old patients with hydronephrosis of different severity showed that the primary factors of the kidney's functional malfunction include not only the obstruction severity and nephrosclerosis grade, but also the residual functioning tissue amount (FTA) of kidneys, which is quantitatively measured in the process of nephroscintigraphy; this helps to assess functional reserves of the renal parenchyma in such patients and prognosticate the disease course (Fig. 18.5).

Thus, use of nephroscintigraphy helps to significantly speed the pediatric patient's examination up, accurately measure the functionally active renal parenchyma amount present at various pathological forms in children regardless of age, significantly optimize outcome prognosis, and reduce risk of chronic renal failure.

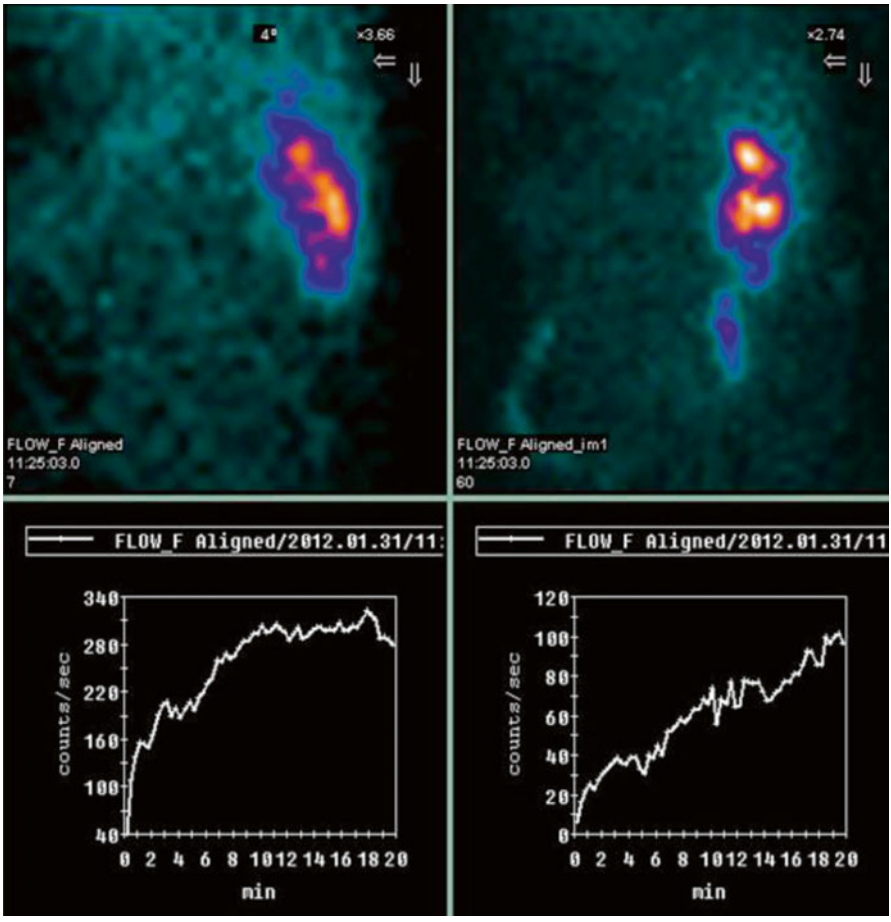

Fig. 18.5 Patient A., 11 years of age. Hydronephrosis of the only – right – kidney. Condition after left-sided nephrectomy. Gamma-ray images – significant decrease in the functioning tissue amount, low secretory-excretory function, urodynamic disorders. Risk group patient

18.5 Radionuclide Hepatography

Radionuclide hepatography using ^{99m}Tc technephyte (37–150 MBq) is an organ-specific method of examining absorption-excretory function of hepatocytes and biliary tract patency. Dynamic 1–1.5-h-long examination of liver helps to detect the slightest deviations in the hepatocyte function, specify the type of jaundice, distinguish between active and non-active forms of hepatitis, and determine prognosis of the disease (Figs. 18.6, 18.7, and 18.8).

It ought to be mentioned that quantitative analysis of activity/time curves of the "interest zones" obtained by means of hepatobiliary scintigraphy helps to comprehensively assess concentration and motor function of the gallbladder, determine occurrence of bile reflux to stomach and patency of biliary tracts, detect incompetence of the sphincter of Oddi or the sphincter of Lutkens, specify occurrence of cholestasis, and qualify morphological condition of the liver

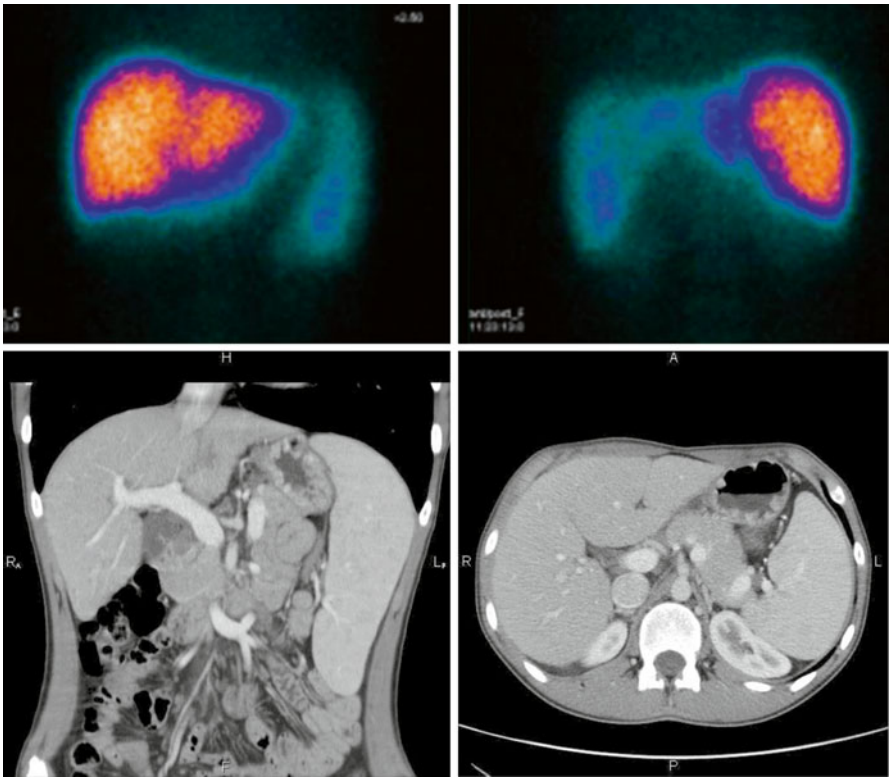

Fig. 18.6 Patient L., 10 years of age. Hepatoscintigraphy: chronic hepatitis. Liver enlargement, uneven colloid distribution, marked splenomegaly, spleen RP accumulation exceeds the norm by 15 %. *Below*: the same patient (L., 10 years of age): axial computed tomograms (*right*) and frontal image reconstruction (*left*). Chronic hepatitis. Diffuse liver enlargement, normal shape, sharp and smooth contours. Marked splenomegaly

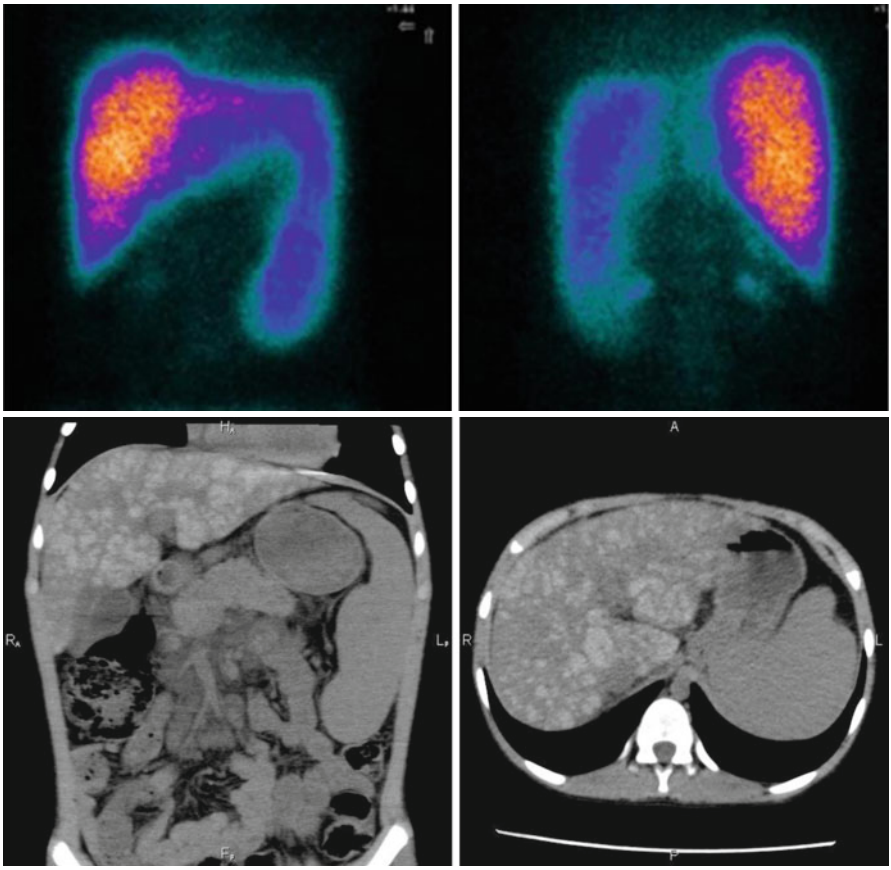

Fig. 18.7 Patient K., 13 years of age. Hepatoscintigraphy: developed hepatic cirrhosis, altered shape of the organ, markedly uneven (spotty) RP distribution, splenomegaly, high spleen RP accumulation. *Below*: the same patient (K., 13 years of age): axial computed tomograms (*right*) and frontal image reconstruction (*left*). Hepatic cirrhosis, segmental liver contours, liver enlargement. Uneven structure with multiple regenerative nodes. Cobblestone appearance. Leveled hepatic vascular pattern. Splenomegaly

and the gallbladder, as well as of extrahepatic bile ducts (internally). Along with that, CT and scintigraphy complement each either at some forms of hepatic pathologies and ensure excellent diagnostic effect (Figs. 18.9, 18.10, 18.11, and 18.12).

18.6 Radionuclide Cardiac Pathology Diagnosis

Radionuclide cardiac pathology diagnosis in children consists in perfusion myocardial scintigraphy by means of selective ^{99m}Tc technetril set (250–550 MBq) accumulation in the myocardium. It involves measurement of the left ventricular (LV) end-systolic and end-diastolic volume, as well as ejection fraction, determination of the LV wall's hypo- or dyskinesia zones, assessment of the LV walls' motility and

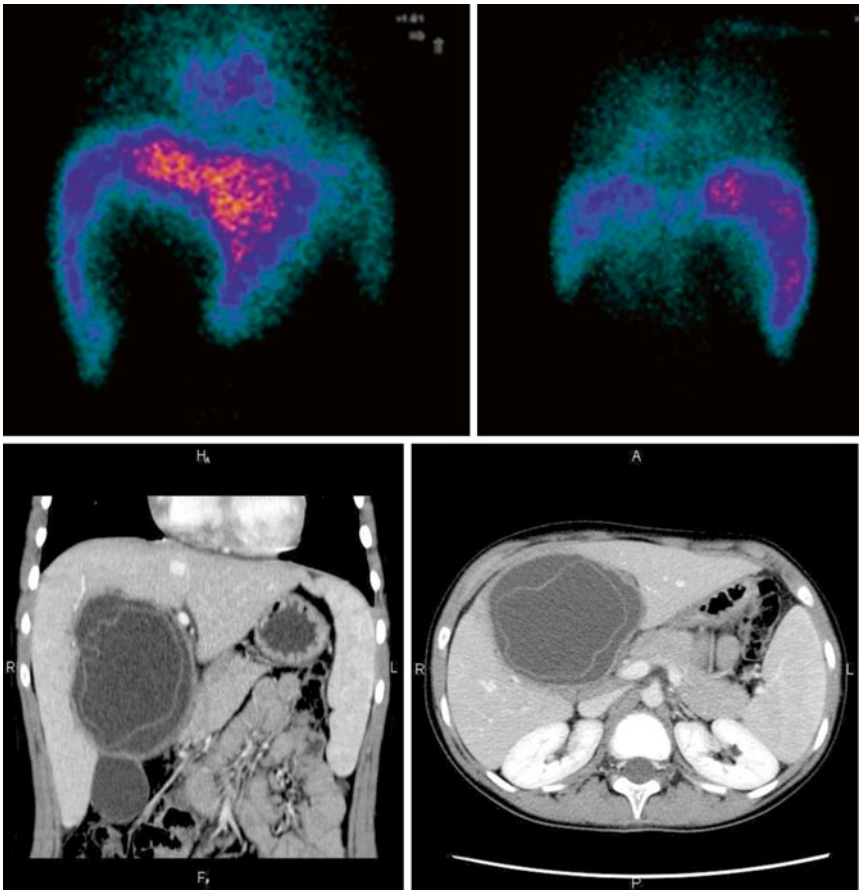

Fig. 18.8 Patient M., 11 years of age. Hepatoscintigraphy at a focal liver lesion: developed hydatid of the right hepatic lobe: altered colloid distribution and shape of the organ, significant singular RP accumulation defect in the form of a "cold" focus with sharp contours. *Below*: the same patient (M., 11 years of age): axial computed tomograms (*right*) and frontal image reconstruction (*left*): hydatid of the right hepatic lobe, slight liver enlargement. Large unicameral cyst with thickened conspicuous capsule and internal content with linear barriers in the parenchyma of liver segments IV and VIII. No symptoms of capsule calcination

the systolic/diastolic ratio and three-dimensional analysis of tomographic heart slices, as well as analysis of the perfusion map and volume/time curves. The examination may also involve radiocardiography (RCG) based on the curve recording of the radiotracer's blood circulation parameters.

It is also important to mention that, unlike other methods, radionuclide diagnosis allows directly examining a heart under stress (physical or psychological) and prognosticating the result of such a stress exposure, i.e., the patient's or the young sportsman's possible future (Fig. 18.13).

Perfusion myocardial scintigraphy holds a special place in diagnosing various forms of cardiomyopathies in children; this process requires analyzing the perfusion map and volume/time curves (Fig. 18.14).

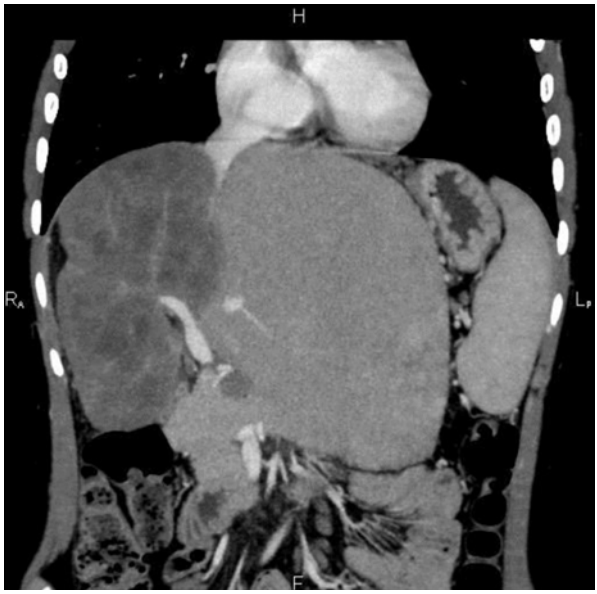

Fig. 18.9 Patient M., 10 years of age. Frontal liver intravenous contrast-enhanced computed tomography: chronic Budd-Chiari syndrome. Compensated ischemic hepatic cirrhosis. Significant disproportion of liver segments, marked caudate lobe enlargement. Thinned branches of the hepatic artery and the portal vein, smaller amount and order thereof

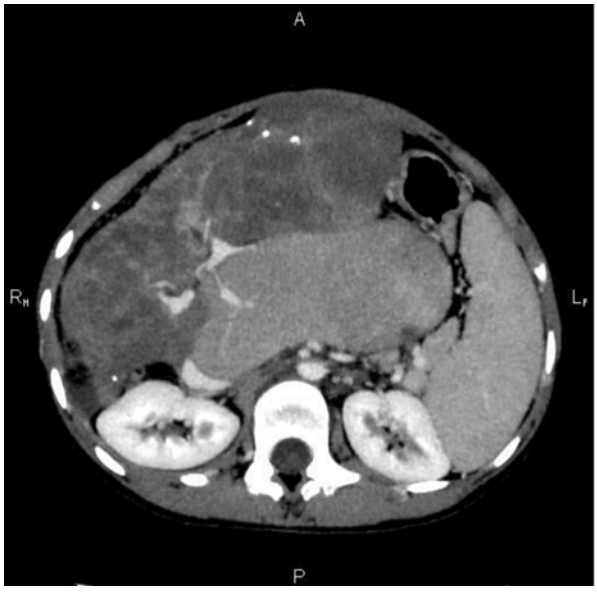

Fig. 18.10 The same patient (M., 10 years of age). Axial liver intravenous contrast-enhanced computed tomography: diffuse focal hepatic parenchyma alterations, calcificates. High occlusion of hepatic veins (visualized in the ostial projection). Deformed and narrowed lumen of the liver segment of the inferior vena cava

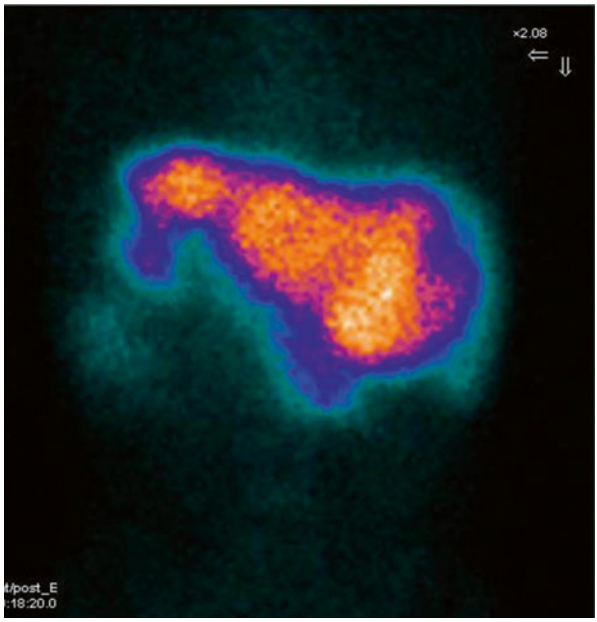

Fig. 18.11 Patient M., 10 years of age. Chronic Budd-Chiari syndrome. Static hepatoscintigraphy (^{99m}Tc technephyte) – 07.06.2013. Frontal projection. Large RP accumulation defects with sharp contours (tissue necrosis foci). Significant size reduction of the right lobe, enlargement of the left lobe

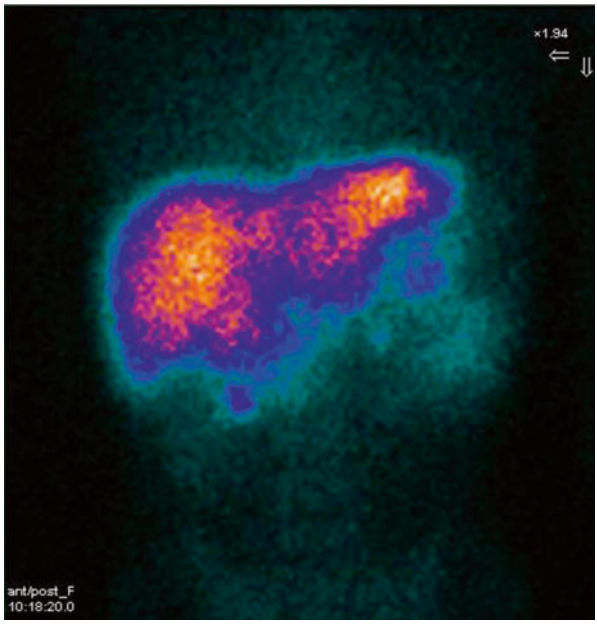

Fig. 18.12 The same patient (M., 10 years of age). Static hepatoscintigraphy (^{99m}Tc technephyte) – 07.06.2013. Posterior projection. Large RP accumulation defects with sharp contours (tissue necrosis foci). Significant size reduction of the right and portal lobe, significant enlargement of the left lobe

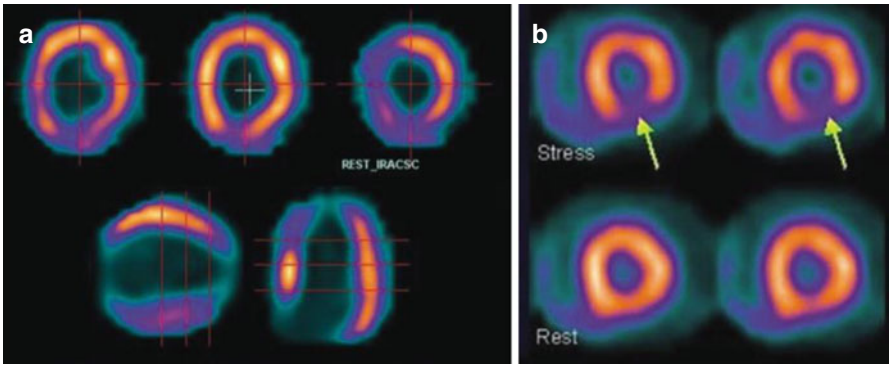

Fig. 18.13 (**a**) Tomographic heart slices obtained with ECG-synchronized perfusion SPECT for visual assessment of the left ventricular myocardium in three projections (examination of sportsman S., 16 years of age). (**b**) Tomographic heart slices (examination of sportsman S., 16 years of age) obtained at the stress test peak: temporary RP accumulation defect in the left ventricular inferior wall (hypoperfusion zone) at physical stress (shown with *arrows*); no defect at rest

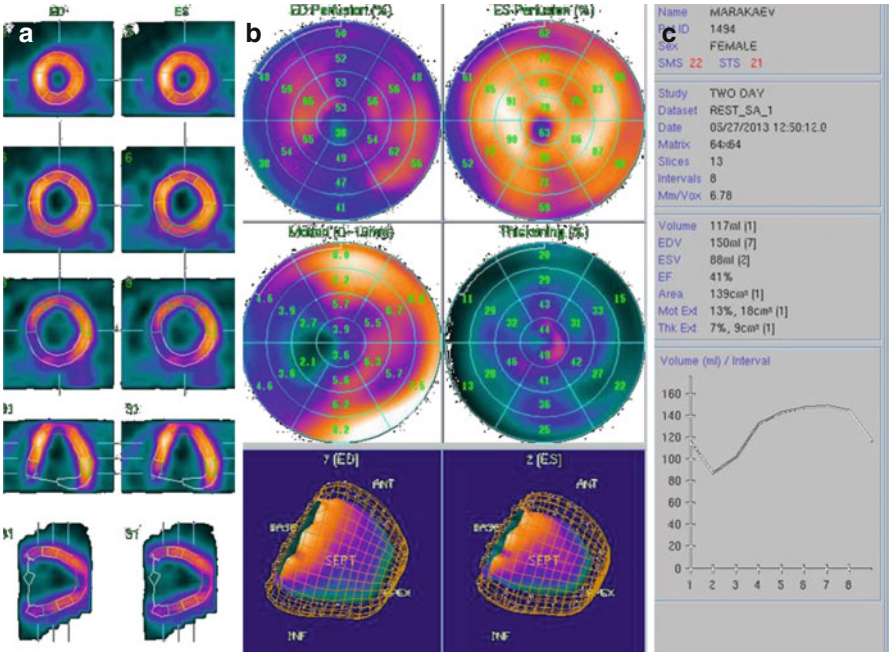

Fig. 18.14 Patient M., 13 years of age. Tomographic slices (**a**), perfusion map (**b**), and volume/time curve (**c**) at dilatation cardiomyopathy: (**a**) tomographic slices in three projections. LV cavity widening. Visualization of moderate hypoperfusion zones in basal segments of the anterior wall and mid-basal segments of the inferior wall. (**b**) *1* and *2* – "bovine eye" – diastolic and systolic perfusion. Not previously mentioned alterations: deep and small-area hypoperfusion focus with pharmaceutic accumulation decrease by more than 60 % (cardiosclerosis or ischemia); *3* LV walls' motility. Uneven left ventricular contractile function, the most marked hypokinesis is observed in the IVS area. (**c**) Low ejection fraction (41 %; according to the automatic software data processing); end-diastolic (*EDV*) and end-systolic (*ESV*) volume curves – late diastolic stage impairments

Thus, radionuclide diagnosis provides unique possibilities for examining condition and heart blood supply in children of different age.

18.7 Radionuclide Pulmonary Pathology Diagnosis

Radionuclide pulmonary pathology diagnosis in children helps to assess such important parameters as pulmonary ventilation, external respiration condition, bronchial patency, and physiological lesser circulation disorders. Perfusion pulmonary scintigraphy (pulmonary gamma-ray imaging) is performed by means of intravenous administration of RP – ^{99m}Tc macrotech (70–200 MBq) – and subsequent registration of a lung image by means of a gamma-ray chamber. Images are taken in the anteroposterior and the posterior-anterior projection (Figs. 18.15 and 18.16).

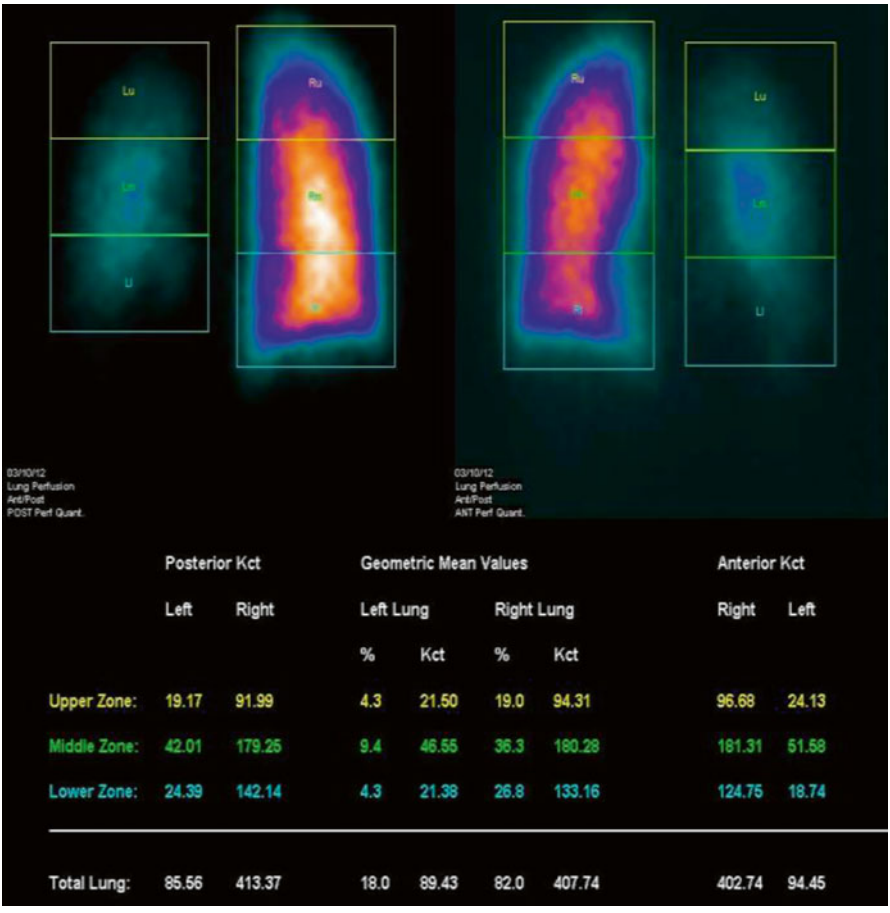

	Posterior Kct		Geometric Mean Values				Anterior Kct	
	Left	Right	Left Lung		Right Lung		Right	Left
			%	Kct	%	Kct		
Upper Zone:	19.17	91.99	4.3	21.50	19.0	94.31	96.68	24.13
Middle Zone:	42.01	179.25	9.4	46.55	36.3	180.28	181.31	51.58
Lower Zone:	24.39	142.14	4.3	21.38	26.8	133.16	124.75	18.74
Total Lung:	85.56	413.37	18.0	89.43	82.0	407.74	402.74	94.45

Fig. 18.15 Perfusion scintigraphy. Patient D., 14 years of age. Hypoplasia of the left lung

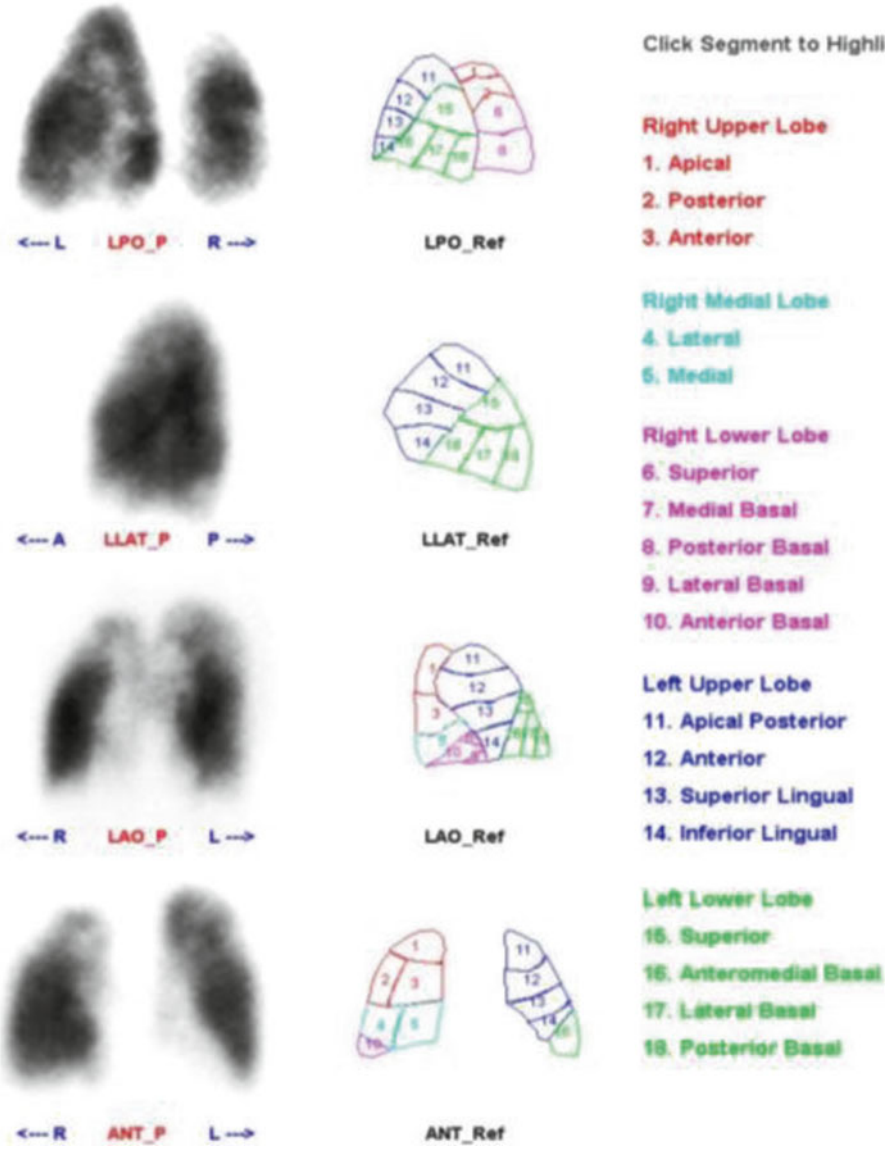

Fig. 18.16 Pulmonary gamma-ray imaging. Patient O., 15 years of age. Focal alterations in both lungs

The "interest zones" selected for processing pulmonary gamma-ray images are upper, middle, and lower segments of each kidney. Normally, RP accumulation degree increases evenly from lung apices to lung bases, as seen in gamma-ray images, while the radionuclide accumulation difference between lung segments

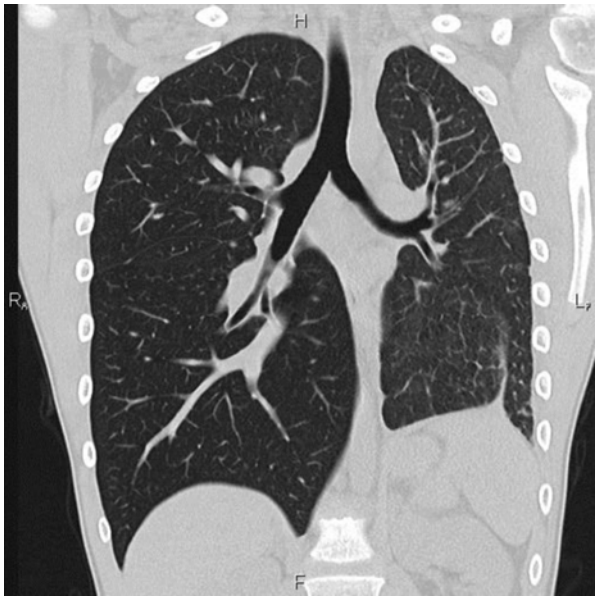

Fig. 18.17 Patient G., 12 years of age. Spiral chest CT. Congenital lung malformation: hypoplasia of the left lung. Frontal MPR reconstruction, pulmonary window. Left lung volume reduction, left mediastinal displacement. Abnormal angioarchitecture of the left lung, thinned and deformed pulmonary vessels, decreased number of bronchial branches, thickened peribronchial interstitium. Compensatorily increased airness of the contralateral lung

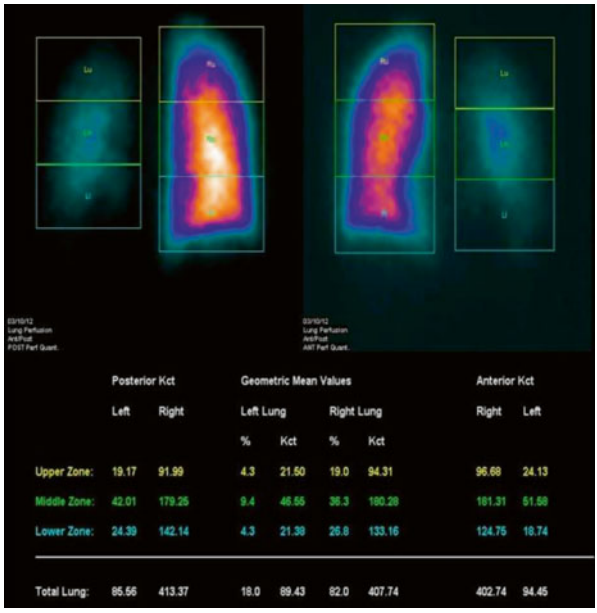

Fig. 18.18 The same patient (G., 12 years of age). Pulmonary gamma-ray imaging: hypoplasia of the left lung: frontal projection (*right*) and posterior projection (*left*)

does not exceed 5–7 %. Hybrid gamma-ray images of a pediatric patient with right lung hypoplasia and a healthy peer are given for comparison in Figs. 18.17, 18.18, and 18.19.

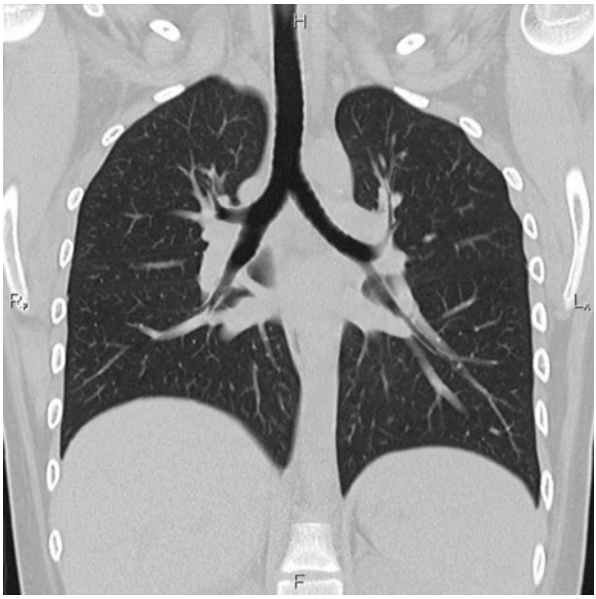

Fig. 18.19 Generally healthy child, 12 years of age. Normal spiral chest CT. Deformity in the frontal projection, pulmonary window

18.8 Radionuclide Skeletal System Pathology Diagnosis

Radionuclide skeletal system pathology diagnosis in children is performed at multiprofile pediatric inpatient hospitals far more rarely than other methods. The principal instrumental methods of diagnosing bone diseases are radiography and CT. They detect bone tissue demineralization, fractures, and pseudofractures well. However, such pathological forms as osteopenia are visible in regular radiograms only when 30–50 % of the bone mass has been lost. In this context, CT is more informative. Along with that, bone scintigraphy is used at several forms of inflammatory (osteomyelitis) or metabolic bone tissue pathologies or at rare diseases in children; it consists in administration of ^{99m}Tc technefor (250–550 MBq depending on the indication) to the patient and radionuclide examination several hours after RP accumulation in the bon tissue, which helps to detect metabolically active hyperfixation foci (Fig. 18.20). It ought to be mentioned that bone scintigraphy is an irreplaceable primary method of detecting skeletal metastases, especially in

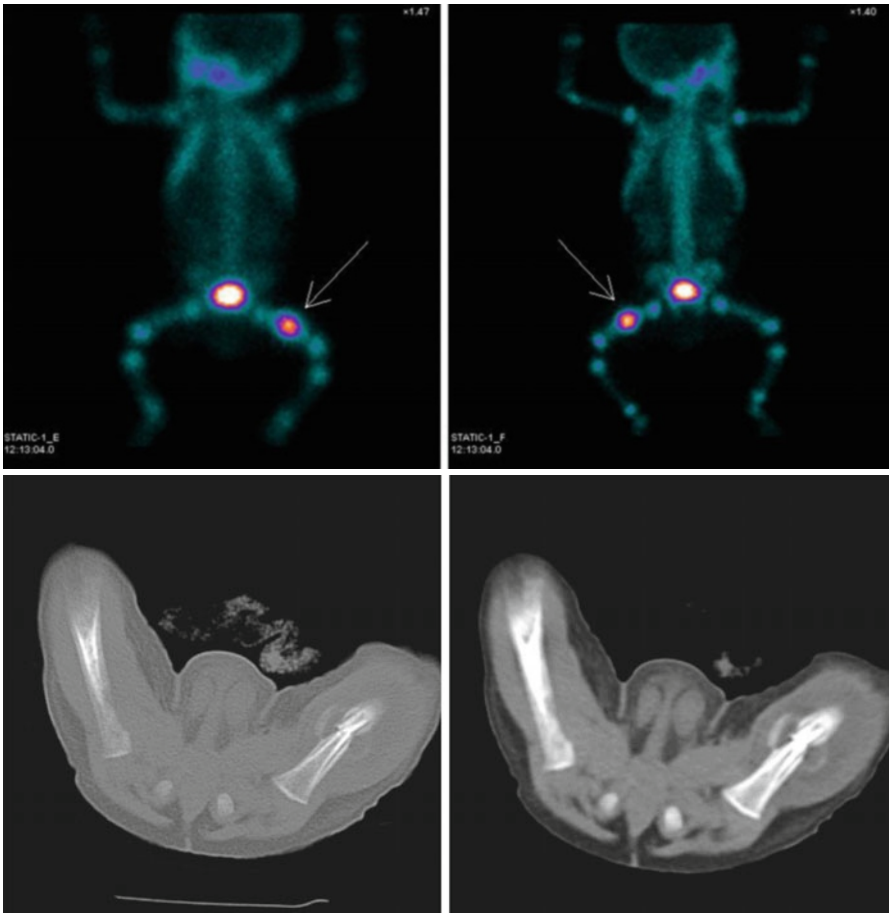

Fig. 18.20 Patient P., 15 years of age. *Above*: bone scintigraphy: RP accumulation in the inflammatory zone at osteomyelitis of the left femoral bone (*arrow*). *Below*: the same patient; CT, modes "soft tissue window" (*right*) and "bone window" (*left*): damaged bone tissue of the left femoral bone

patients with severe bone metastatic disease. Use of CT and MRI as diagnostic methods is not cost-effective in the event of such pathological forms; scintigraphy is significantly more sensitive and allows visualizing the whole skeleton (Fig. 18.21).

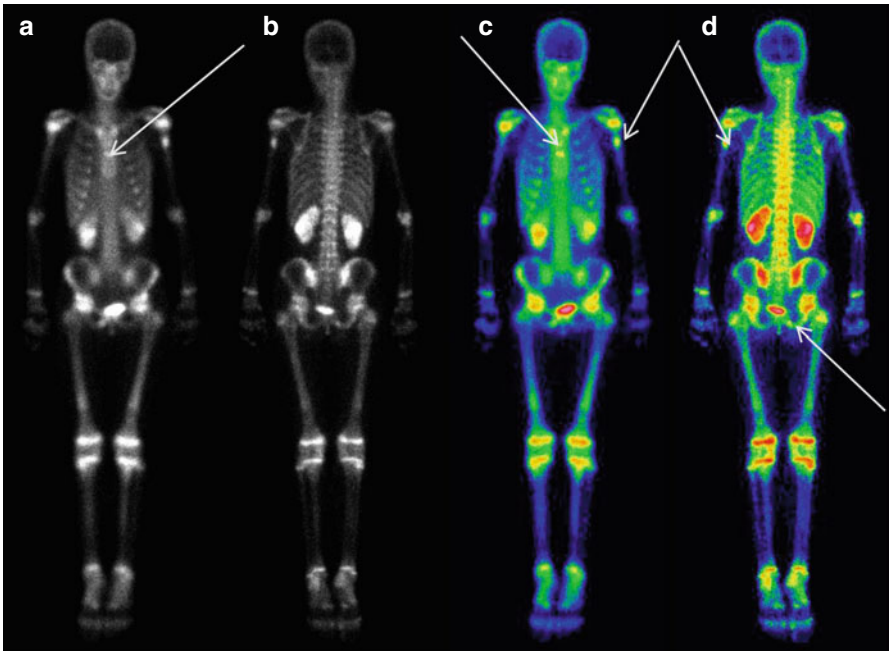

Fig. 18.21 Patient M., 13 years of age. Bone scintigraphy at hemoblastosis: increased RP accumulation foci in the proximal diaphysis of the left humerus (*arrow-**d***), the breastbone (*arrows-**b,c***), and the right ischium (*arrow*). (**a**, **c**) Frontal projection; (**b**, **d**) posterior projection

Conclusion

Nowadays, there exists an algorithm of prescribing imaging methods in pediatrics. Without any doubt, ultrasonography is a sort of basis of screening radiodiagnosis. In most cases, USD helps to reveal pathological alterations of organs and establish correct diagnosis. Along with that, USD helps to detect patients requiring auxiliary examination with high-technology equipment. The main advantages of USD are high availability, low cost, and absence of radiation exposure. Another valuable property is the ability to immediately determine the blood supply mode of the area under analysis. USD helps to significantly visualize almost all groups of lymph nodes (except for mediastinal lymph nodes). However, one of the method's main disadvantages is that bone tissue and air impede ultrasonic transmission. Along with that, it is widely acknowledged that USD is an operator-dependent method, i.e., diagnostic information directly depends on the physician's qualification and experience.

Routine X-ray diagnosis, which, along with other aspects, is a peculiar type of screening intended to detect various forms of pathologies, especially of the bone tissue and lungs, remains common. Modern X-ray diagnostic systems have completely digitalized; this helped to significantly reduce radiation exposure and increase diagnostic informative value.

Computed tomography represents a new cycle of development, a new generation of radiodiagnosis. In routine radiography images are two-dimensional and linear; they represent summation of all the X-rays that have crossed through the body. In computed tomography, we may see and point within the body. We may obtain not only 3D, but also 4D (animated) images. Modern multislice (multispiral) computed tomographs are super quick and accumulate data in 10 s or faster. Depending on the aims and objectives of the examination, 20–40 % of children require using intravenous contrast enhancement for computed tomography. Contrast enhancement shows dynamic distribution of the contrast medium within the body at different stages: arterial, venous, parenchymatous, and delayed; this helps to differentiate between the pathological processes occurring in the body. CT angiography (from coronary arteries and pulmonary veins to various vascular malformations) has been becoming the gold standard. The principal disadvantage of computed tomography is a rather significant radiation exposure, which usually varies from 1.5 to 10 mSv. This is crucial for a child's body and makes physicians search for alternative examination methods.

Magnetic resonance imaging is a safe and highly effective non-ionizing examination method. It is based on nuclear magnetic resonance in the presence of static magnetic field. Radiofrequency sequences are used to obtain images. The method features high natural tissue contrast. An extremely high space resolution allows detailing the image with anatomic precision. A possibility to selectively suppress water and fat in the images is successfully employed to detect various tissue edemata. Functional MRI methods help to indirectly assess content of specific metabolites (MR spectroscopy), tissue diffusion (DWI and DTI), and metabolic activity of brain segments (f-MRI). However, the method also features restrictions. MRI is banned in certain groups of patients – persons with cardio- or neurostimulators – due to the static magnetic field. Along with that, the examination lasts for a rather long time (usually, 15–40 min) and is associated with loud noise. This makes it hardly possible in the children aged from 2 months to 5 years without anesthesia.

Scintigraphy also holds a place in this algorithm. Possibilities of this method of lifetime imaging of a growing person's pathophysiological and metabolic processes are determined by development of molecular markers (tracers), which would allow assessing distribution of individual molecular targets in tissues of various organs, and new SPECT- and PET-based technologies of functional metabolic mapping at pathologies.

Our experience of such examinations indicates that in order to increase cost-effectiveness of radionuclide diagnosis, a diagnostic imaging algorithm ought to be used at different pathological forms in children of different age; it is also necessary to correctly determine indications to a radionuclide examination and adequately assess prognostic value of the information obtained by a radiologist. A radiologist ought to have an acceptable examination strategy and objective attitude towards the available data in order to use them for diagnostic solutions and ensure high quality of diagnostic procedures.

Suggested Reading

1. Anagnostopoulos CD, Bax JJ, Nihoyannopoulos P, van der Wall E (eds) (2006) Noninvasive imaging of myocardial ischemia. Springer-Verlag London Limited, London, p 314
2. Bailey DL, Townsend DW, Valk PE, Maisey MN (2005) Positron emission tomography – basic sciences. Springer-Verlag London Limited, London, p 382
3. Bayram T, Yilmaz AH, Demir M, Sonmez B (2011) Radiation dose to technologists per nuclear medicine examination and estimation of annual dose. J Nucl Med Technol 39(1):55–59
4. Clevert DA, Stock K, Klein B (2009) Evaluation of Acoustic Radiation Force Impulse (ARFI) imaging and contrast-enhanced ultrasound in renal tumors of unknown etiology in comparison to histological findings. Clin Hemorheol Microcirc 43(1):95–107
5. Dacher JN, Hitzel A, Avni FE, Vera P (2005) Imaging strategies in pediatric urinary tract infection. Eur Radiol 15(7):1283–1288
6. Fahey FH, Treves ST, Adelstein SJ (2012) Minimizing and communicating radiation risk in pediatric nuclear medicine. J Nucl Med Technol 40(1):13–24
7. FJTh W, Bruni W, Zaret BL (2004) Nuclear cardiology, the basics: how to set up and maintain a laboratory, Contemporary cardiology. Humana Press Inc, Totowa, p 298
8. Green MA, Hutchins GD (2011) Positron emission tomography (PET) assessment of renal perfusion. Semin Nephrol 31(3):291–299
9. Grenier N, Quaia E, Prasad PV, Juillard L (2011) Radiology imaging of renal structure and function by computed tomography, magnetic resonance imaging, and ultrasound. Semin Nucl Med 41(1):45–60
10. Krishnamurthy GT, Krishnamurthy S (2009) Nuclear hepatology. A textbook of hepatobiliary diseases, 2nd edn. Springer, Berlin/Heidelberg, p 365
11. Mahmarian JJ, Chang S, Nabi F (2014) Nuclear cardiology: 2014 innovations and developments. Methodist Debakey Cardiovasc J 10(3):163–171
12. Mohammadjafari H, Aalaee A, Salehifar E et al (2011) Doppler ultrasonography as a predictive tool for permanent kidney damage following acute pyelonephritis: comparison with dimercaptosuccinic acid scintigraphy. Iran J Kidney Dis 5(6):386–391
13. Muoz JJ, Ribes R (2010) Learning vascular and interventional radiology. Springer-Verlag London Limited, London, p 264
14. Renard-Penna R, Marcy PY, Lacout A, Thariat J (2012) Imaging of the kidney. Bull Cancer 99(3):251–262
15. Routh JC, Grant FD, Kokorowski PJ et al (2012) Economic and radiation costs of initial imaging approaches after a child's first febrile urinary tract infection. Clin Pediatr (Phila) 51(1):23–30
16. Shyn PB (2013) Interventional positron emission tomography/computed tomography: state-of-the-art. Tech Vase Interv Radiol 16(3):182–190
17. Treves ST, Falone AE, Fahey FH (2014) Pediatric nuclear medicine and radiation dose. Semin Nucl Med 44(3):202–209
18. Vivier PH, Dolores M, Le Cloirec J et al (2011) Imaging evaluation of renal function: principles and limitations. J Radiol 92(4):280–290
19. Won KS, Song BI (2013) Recent trends in nuclear cardiology practice. Chonnam Med J 49(2):55–64
20. Zucchetta P, Artifoni L, Rigamonti W, Cecchin D, Bui F, Murer L (2010) Molecular biology and nuclear medicine in pediatric hydronephrosis. Q J Nucl Med Mol Imaging 54(4):363–371